**Geomechanics and Engineering**, *Vol. 17, No. 2 (2019) 175-180*
DOI: https://doi.org/10.12989/gae.2019.17.2.175


# Analyzing post-buckling behavior of continuously graded FG nanobeams with geometrical imperfections

Ridha A. Ahmed, Raad M. Fenjan and Nadhim M. Faleh*

*Al-Mustansiriyah University, Engineering College P.O. Box 46049, Bab-Muadum, Baghdad 10001, Iraq*

*(Received October 20, 2018, Revised December 11, 2018, Accepted January 9, 2019)*

**Abstract.** This research is concerned with post-buckling investigation of nano-scaled beams constructed from porous functionally graded (FG) materials taking into account geometrical imperfection shape. Hence, two types of nanobeams which are perfect and imperfect have been studied. Porous FG materials are classified based on even or uneven porosity distributions. A higher order nonlinear refined beam theory is used in the present research. Both perfect and imperfect nanobeams are formulated based on this refined theory. A detailed study is provided to understand the effects of geometric imperfection, pore distribution, material distribution and small scale effects on buckling of FG nanobeams.

**Keywords:** post-buckling; refined beam theory; porous nanobeam; nonlocal elasticity; porosities

## 1. Introduction

In a FG material, all material properties may change from one side to another side by means of a prescribed distribution (Ebrahimi and Barati 2017). These two sides may be ceramic or metal. Mechanical characteristics of a FG material can be described based on the percentages of ceramic and metal phases. The material distribution in FG materials may be characterized via a power-law function (Barati *et al.* 2016, 2017). FG materials are not always perfect because of porosity production in them (Chen *et al.* 2015). Existence of porosities in the FG materials may significantly change their mechanical characteristics. For example, the elastic moduli of porous FG material is smaller than that of perfect FG material. Up to now, many authors focused on wave propagation, vibration and buckling analyzes of FG structures having porosities (Wattanasakulpong and Ungbhakorn 2014, Yahia *et al.* 2015, Hadji *et al.* 2015, Atmane *et al.* 2015, Barati 2017, Mirjavadi *et al.* 2019).

At nano scale, size effects are prominent and must be evaluated in order to accurate analyzes of nano-scale structures. Therefore, classical elasticity is not adequate for analyzes of nano-scale structures. A refined elasticity theory called nonlocal theory of Eringen (1983) may be used for static and dynamic analysis of structures at nano-scale. Most of researches on static and dynamic analysis of structures at nano-scale deals with nonlocal elasticity having one scale parameter. Nonlocal elasticity containing scale parameter called nonlocal parameter is previously employed in many investigations on nano-sized beams and plates (Berrabah *et al.* 2013, Zhang *et al.* 2014, Belkorissat *et al.* 2015, Zemri *et al.* 2015, Bouderba *et al.* 2016, Li *et al.* 2016, Li and Hu 2017, Ebrahimi and Barati 2018, Barati and Zenkour 2018a, b). These researches show a significant change in mechanical behavior of nano-structures when the scale parameter is involved.

The present article is concerned with post-buckling investigation of nano-scaled beams constructed from porous functionally graded (FG) materials taking into account geometrical imperfection shape. Therefore, two types of nanobeams which are perfect and imperfect have been studied. Porous FG materials are classified based on even or uneven porosity distributions. A higher order nonlinear refined beam theory is used in the present research. Both perfect and imperfect nanobeams are formulated based on this refined theory. A detailed study is provided to understand the effects of geometric imperfection, pore distribution, material distribution and small scale influences.

## 2. FG materials having porosities

The material distribution in FG materials may be characterized via a power-law function (Barati *et al.* 2016, 2017). FG materials are not always perfect because of porosity production in them. Existence of porosities in the FG materials may significantly change their mechanical characteristics. Depending on the type of porosity distribution, the elastic moduli for porous FG material can be expressed in the following power-law form having material gradient index $p$ as

$$E(z) = (E_c - E_m)\left(\frac{z}{h}+\frac{1}{2}\right)^p + E_m - (E_c + E_m)\frac{\xi}{2} \quad (1a)$$

for even porosities

*Corresponding author, Professor
E-mail: dr.nadhim@uomustansiriyah.edu.iq


http://www.techno-press.org/?journal=gae&subpage=7
ISSN: 2005-307X (Print), 2092-6219 (Online)

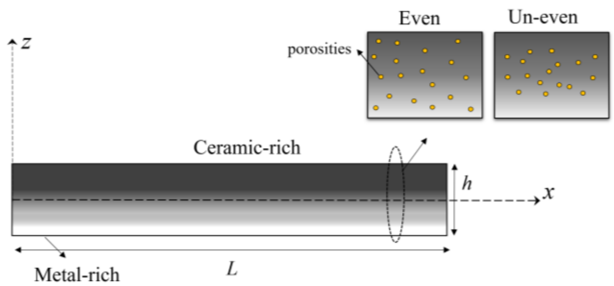


Fig. 1 A FG nanobeam with porosities

$$E(z)=\left(E_c-E_m\right)\left(\frac{z}{h}+\frac{1}{2}\right)^p+E_m-\frac{\xi}{2}\left(E_c+E_m\right)(1-\frac{2|z|}{h}) \quad (1b)$$

for uneven porosities

where $m$ and $c$ corresponds to the metal and ceramic sides, respectively; $\xi$ is the porosity volume fraction. A porous FG nanobeam with length L is shown in Fig. 1.

By defining exact location of neutral axis, the displacement components based on axial $u$, bending $w_b$ and shear $w_s$ displacements may be introduced as

$$u_1\left(x,z\right)=u\left(x\right)-(z-z^*)\frac{\partial w_b}{\partial x}-[f(z)-z^{**}]\frac{\partial w_s}{\partial x} \quad (2a)$$

$$u_3(x,z)=w(x)=w_b(x)+w_s(x) \quad (2b)$$

Here, third order shear function is employed as

$$f(z)=-\frac{z}{4}+\frac{5z^3}{3h^2} \quad (3)$$

and

$$z^*=\frac{\int_{-h/2}^{h/2}E(z)\,zdz}{\int_{-h/2}^{h/2}E(z)\,dz}, \quad z^{**}=\frac{\int_{-h/2}^{h/2}E(z)\,f(z)dz}{\int_{-h/2}^{h/2}E(z)\,dz} \quad (4)$$

According to the non-linear refined beam model, governing equations may be obtained via the procedure presented by Barati and Zenkour (2018a) as

$$\frac{\partial N_x}{\partial x}=0 \quad (5)$$

$$\frac{\partial^2 M_x^b}{\partial x^2}=-\tilde{N} \quad (6)$$

$$\frac{\partial^2 M_x^s}{\partial x^2}+\frac{\partial Q_{xz}}{\partial x}+\tilde{N}=0 \quad (7)$$

in which $N_x$, $M^b$ and $M^s$ are axial, bending and shear moments respectively and

$$\tilde{N}=\frac{\partial}{\partial x}(N_x\frac{\partial(w_b+w_s)}{\partial x}) \quad (8)$$

Here, a refined elasticity theory called nonlocal theory of Eringen (1983) may be used for static and dynamic analysis of beams at nano-scale. Most of researches on static/dynamic analyzes of a structure at nano-scale deals with nonlocal elasticity having one scale parameter ($\mu$). Nonlocal elasticity containing a scale parameter is employed based on the following stress-strain relation

$$\sigma_{xx}-\mu\frac{\partial^2\sigma_{xx}}{\partial x^2}=E(z)\varepsilon_{xx} \quad (9)$$

$$\sigma_{xz}-\mu\frac{\partial^2\sigma_{xz}}{\partial x^2}=G(z)\gamma_{xz} \quad (10)$$

where $\varepsilon_{xx}$ and $\gamma_{xz}$ are axial and shear strains respectively. The axial, bending and shear moments in Eqs. (5)-(7) can be expressed in the following form with the help of Eqs. (9) and (10) as

$$N_x=A[\frac{\partial u}{\partial x}+\frac{1}{2}(\frac{\partial(w_b+w_s)}{\partial x})^2-\frac{1}{2}(\frac{\partial(w_b^*+w_s^*)}{\partial x})^2] \quad (11)$$

$$M_x^b=-D(\frac{\partial^2 w_b}{\partial x^2}-\frac{\partial^2 w_b^*}{\partial x^2})-E(\frac{\partial^2 w_s}{\partial x^2}-\frac{\partial^2 w_s^*}{\partial x^2})+\mu(-N_x\frac{\partial^2(w_b+w_s)}{\partial x^2}) \quad (12)$$

$$M_x^s=-E(\frac{\partial^2 w_b}{\partial x^2}-\frac{\partial^2 w_b^*}{\partial x^2})-F(\frac{\partial^2 w_s}{\partial x^2}-\frac{\partial^2 w_s^*}{\partial x^2})+\mu(-N_x\frac{\partial^2(w_b+w_s)}{\partial x^2}-\frac{\partial Q_{xz}}{\partial x}) \quad (13)$$

$$(1-\mu\nabla^2)Q_{xz}=A_s\frac{\partial w_s}{\partial x} \quad (14)$$

then

$$\begin{aligned}&A=\int_{-h/2}^{h/2}E(z)\,dz,\;\; D=\int_{-h/2}^{h/2}E(z)(z-z^*)^2\,dz,\;\; E=\int_{-h/2}^{h/2}E(z)(z-z^*)(f-z^{**})\,dz\\&F=\int_{-h/2}^{h/2}E(z)(f-z^{**})^2\,dz,\quad A_s=\int_{-h/2}^{h/2}\frac{E(z)}{2(1+v)}g^2dz\end{aligned} \quad (15)$$

Then, inserting Eqs.(11)-(14) into the governing Eqs.(5)-(7) results in this system of equations considering geometric non-linearity and imperfection

$$A(\frac{\partial^2 u}{\partial x^2})+A(\frac{\partial(w_b+w_s)}{\partial x}\frac{\partial^2(w_b+w_s)}{\partial x^2}+\frac{\partial(w_b^*+w_s^*)}{\partial x}\frac{\partial^2(w_b^*+w_s^*)}{\partial x^2})=0 \quad (16)$$

$$-D(\frac{\partial^4 w_b}{\partial x^4}-\frac{\partial^4 w_b^*}{\partial x^4})-E(\frac{\partial^4 w_s}{\partial x^4}-\frac{\partial^4 w_s^*}{\partial x^4})+\frac{\partial}{\partial x}(N_x\frac{\partial w}{\partial x})-\mu\frac{\partial^3}{\partial x^3}(N_x\frac{\partial w}{\partial x})=0 \quad (17)$$

$$\begin{aligned}&-E(\frac{\partial^4 w_b}{\partial x^4}-\frac{\partial^4 w_b^*}{\partial x^4})-F(\frac{\partial^4 w_s}{\partial x^4}-\frac{\partial^4 w_s^*}{\partial x^4})+\frac{\partial}{\partial x}(N_x\frac{\partial w}{\partial x})-\mu\frac{\partial^3}{\partial x^3}(N_x\frac{\partial w}{\partial x})\\&+A_{44}(\frac{\partial^2 w_s}{\partial x^2}-\frac{\partial^2 w_s^*}{\partial x^2})=0\end{aligned} \quad (18)$$

Based on the procedure introduced by Barati and Zenkour (2018a), the axial displacement can be calculated as

$$u=-\frac{1}{2}\int_0^x(\frac{\partial(w_b+w_s)}{\partial x})^2dx+\frac{1}{2}\int_0^x(\frac{\partial(w_b^*+w_s^*)}{\partial x})^2dx+c_1x+c_2 \quad (18)$$

$$u=-\frac{1}{2}\int_0^x(\frac{\partial(w_b+w_s)}{\partial x})^2dx+\frac{1}{2}\int_0^x(\frac{\partial(w_b^*+w_s^*)}{\partial x})^2dx+c_1x+c_2 \quad (19)$$

in which

$$c_2 = 0$$
$$c_1 = \frac{1}{2L}\int_0^L (\frac{\partial(w_b + w_s)}{\partial x})^2 dx - \frac{1}{2L}\int_0^L (\frac{\partial(w_b^* + w_s^*)}{\partial x})^2 dx - \frac{P}{A} \tag{20}$$

where $P$ is applied axial load. By calculating the first derivative of axial displacement, Eqs.(17) and (18) may be re-written as

$$\begin{aligned}&-D(\frac{\partial^4 w_b}{\partial x^4} - \frac{\partial^4 w_b^*}{\partial x^4}) - E(\frac{\partial^4 w_s}{\partial x^4} - \frac{\partial^4 w_s^*}{\partial x^4})\\ &+A[+\frac{1}{2L}\int_0^L (\frac{\partial(w_b + w_s)}{\partial x})^2 dx - \frac{1}{2L}\int_0^L (\frac{\partial(w_b^* + w_s^*)}{\partial x})^2 dx - \frac{P}{A}]\frac{\partial^2 (w_b + w_s)}{\partial x^2}\\ &-\mu A[+\frac{1}{2L}\int_0^L (\frac{\partial(w_b + w_s)}{\partial x})^2 dx - \frac{1}{2L}\int_0^L (\frac{\partial(w_b^* + w_s^*)}{\partial x})^2 dx - \frac{P}{A}]\frac{\partial^4 (w_b + w_s)}{\partial x^4} = 0\end{aligned} \tag{21}$$

$$\begin{aligned}&-E(\frac{\partial^4 w_b}{\partial x^4} - \frac{\partial^4 w_b^*}{\partial x^4}) - F(\frac{\partial^4 w_s}{\partial x^4} - \frac{\partial^4 w_s^*}{\partial x^4}) + A_s(\frac{\partial^2 w_s}{\partial x^2} - \frac{\partial^2 w_s^*}{\partial x^2})\\ &+A[+\frac{1}{2L}\int_0^L (\frac{\partial(w_b + w_s)}{\partial x})^2 dx - \frac{1}{2L}\int_0^L (\frac{\partial(w_b^* + w_s^*)}{\partial x})^2 dx - \frac{P}{A}]\frac{\partial^2 (w_b + w_s)}{\partial x^2}\\ &-\mu A[+\frac{1}{2L}\int_0^L (\frac{\partial(w_b + w_s)}{\partial x})^2 dx - \frac{1}{2L}\int_0^L (\frac{\partial(w_b^* + w_s^*)}{\partial x})^2 dx - \frac{P}{A}]\frac{\partial^4 (w_b + w_s)}{\partial x^4} = 0\end{aligned} \tag{22}$$

## 3. Solution technique

Here, a solution of the above non-linear equations based on the non-linear buckling of a porous nanobeam has been provided. At this step, the lateral/shear deflections must be assumed as

$$w_b = \sum_{m=1}^{\infty} W_{bm} X_m(x) \tag{23a}$$

$$w_s = \sum_{m=1}^{\infty} W_{sm} X_m(x) \tag{23b}$$

where ($W_{bm}$, $W_{sm}$) are buckling amplitudes; $X_m$ is a function in order to introduce boundary edges which are

$$w_b = w_s = 0, \quad \frac{\partial^2 w_b}{\partial x^2} = \frac{\partial^2 w_s}{\partial x^2} = 0 \tag{24a}$$

both ends simply-supported

$$w_b = w_s = 0, \quad \frac{\partial w_b}{\partial x} = \frac{\partial w_s}{\partial x} = 0 \tag{24b}$$

both ends clamped

The imperfection displacements (with amplitude W*) may be introduced as (Emam 2009)

$$\begin{aligned}w_b^* &= W_b^* \Phi(x) = W_b^* \sin\left(\pi \frac{x}{L}\right)\\ w_s^* &= W_s^* \Phi(x) = W_s^* \sin\left(\pi \frac{x}{L}\right)\end{aligned} \tag{25a}$$

both ends simply-supported

$$\begin{aligned}w_b^* &= W_b^* \Phi(x) = 0.5 W_b^* \left(1 - \cos\left(2\pi \frac{x}{L}\right)\right)\\ w_s^* &= W_s^* \Phi(x) = 0.5 W_s^* \left(1 - \cos\left(2\pi \frac{x}{L}\right)\right)\end{aligned} \tag{25b}$$

both ends clamped

After placing Eq. (23) into Eqs. (21)-(22), implementation of Galerkin's approach yields

$$k_{1,1} W_{bm} + k_{1,2} W_{sm} + G^* \tilde{W}^3 + \Psi_{1,1} W_b^* + \Psi_{1,2} W_s^* = 0 \tag{26a}$$

$$k_{2,1} W_{bm} + k_{2,2} W_{sm} + G^* \tilde{W}^3 + \Psi_{2,1} W_b^* + \Psi_{2,2} W_s^* = 0 \tag{26b}$$

in which $\tilde{W} = W_{bm} + W_{sm}$ and

$$k_{1,1} = -D\Upsilon_{40} - P\Upsilon_{20} + \mu P\Upsilon_{40} - \frac{A}{2L}\left(W_b^*\right)^2 \int_0^L (\Phi')^2 dx \Upsilon_{20} + \mu \frac{A}{2L}\left(W_b^*\right)^2 \int_0^L (\Phi')^2 dx \Upsilon_{40} \tag{27a}$$

$$k_{1,2} = -E\Upsilon_{40} - P\Upsilon_{20} + \mu P\Upsilon_{40} - \frac{A}{2L}\left(W_b^*\right)^2 \int_0^L (\Phi')^2 dx \Upsilon_{20} + \mu \frac{A}{2L}\left(W_b^*\right)^2 \int_0^L (\Phi')^2 dx \Upsilon_{40} \tag{27b}$$

$$\begin{aligned}k_{2,2} &= -F\Upsilon_{40} + A_s\Upsilon_{20} - P\Upsilon_{20} + \mu P\Upsilon_{40}\\ &- \frac{A}{2L}\left(W_s^*\right)^2 \int_0^L (\Phi')^2 dx \Upsilon_{20} + \mu \frac{A}{2L}\left(W_s^*\right)^2 \int_0^L (\Phi')^2 dx \Upsilon_{40}\end{aligned} \tag{27c}$$

$$G^* = A(\frac{1}{2L}\Upsilon_{11}\Upsilon_{20}) - \mu A(\frac{1}{2L}\Upsilon_{11}\Upsilon_{40}) \tag{27d}$$

$$\Psi_{1,1} = D\int_0^L \Phi^{(4)} X_m dx \tag{27e}$$

$$\Psi_{1,2} = \Psi_{2,1} = E\int_0^L \Phi^{(4)} X_m dx \tag{27f}$$

$$\Psi_{2,2} = F\int_0^L \Phi^{(4)} X_m dx - A_s \int_0^L \Phi^{(2)} X_m dx \tag{27g}$$

and

$$\{\Upsilon_{00}, \Upsilon_{20}, \Upsilon_{40}, \Upsilon_{11}\} = \int_0^L \{X_m X_m, X_m'' X_m, X_m'''' X_m, X_m' X_m'\} dx$$
$$\{\Upsilon_{0000}, \Upsilon_{1100}, \Upsilon_{2000}\} = \int_0^L \{X_m X_m X_m X_m, X_m' X_m' X_m X_m, X_m'' X_m X_m X_m\} dx$$

Based on above discussion, the function $X_m$ may be selected as

$$\text{S-S:} \quad X_m(x) = \sin(\tfrac{m\pi}{L}x) \tag{28}$$

$$\text{C-C:} \quad X_m(x) = 0.5(1 - \cos(\tfrac{2m\pi}{L}x)) \tag{29}$$

The presented results are based on the following dimensionless nonlocal parameter

$$\mu = \frac{e_0 a}{L} \tag{30}$$

## 4. Results and discussions

This section is concerned with post-buckling investigation of nano-scaled beams constructed from porous FG materials taking into account geometrical imperfection shape. Hence, two types of nanobeams which are perfect and imperfect have been studied. Porous FG materials are

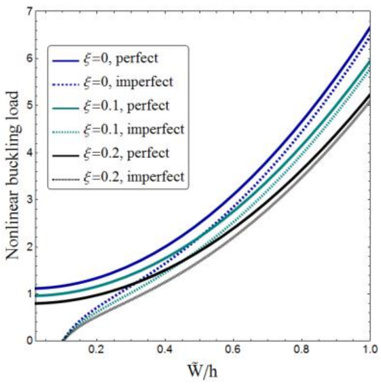


(a) S-S

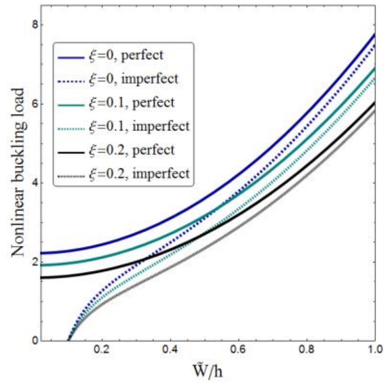


(b) C-C

Fig. 2 Nonlinear buckling path of the nanobeam against normalized deflection for different uniform pore parameters (*L*/*h*=10, *p*=1, *μ*=0.2)

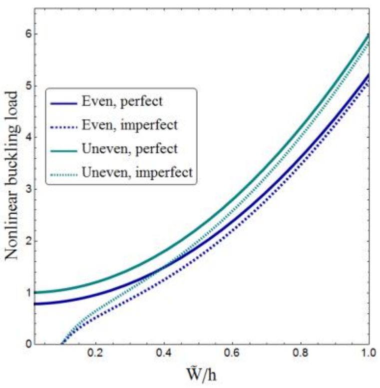


(a) *p*=1

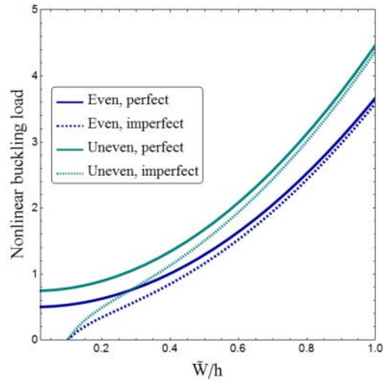


(b) *p*=2

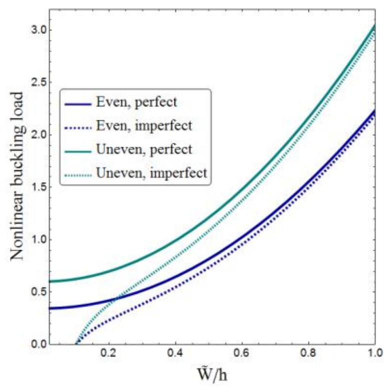


(c) *p*=5

Fig. 3 Nonlinear buckling path of the nanobeam against normalized deflection for various pore distributions (*L*/*h*=10, *μ*=0.2, *ξ*=0.2).

classified based on even or uneven porosity distributions. Both perfect and imperfect nanobeams are formulated based on a higher order refined beam theory. A detailed study is provided to understand the effects of geometric imperfection, pore distribution, material distribution and small scale effects on buckling of FG nanobeams. To this end, two material phases are selected as:

- $E_c = 380\ GPa,\ \rho_c = 3800\ kg/m^3,\ v_c = 0.3$
- $E_m = 70\ GPa,\ \rho_m = 2707\ kg/m^3,\ v_m = 0.3$

Fig. 2 indicates the impact of pore parameter on non-linear buckling curves of geometrically imperfect/perfect porosity-dependent nano-sized beams when *L*=10h and $W^*/h=0.1h$ based on even pore dispersion. Different amounts of pore parameter have been selected (*ξ*=0, 0.1 and 0.2). In the case of ideal (perfect) nano-sized beams, the beginning point ($\tilde{W}/h=0$) denotes the bifurcation buckling point. However, for the state of imperfect nano-sized beams, no critical point exists, because the nano-sized beams are rested in their initial configurations. One can find that the non-linear buckling loads become greater by increasing in non-dimensional maximum deflection highlighting the intrinsic stiffening influence related to geometrical non-linearity. Then, one can find that increasing in pore parameter yields a lower buckling load in the case of ideal or imperfect nano-sized beams. The reason comes from the reduction of nano-sized beam stiffness with the

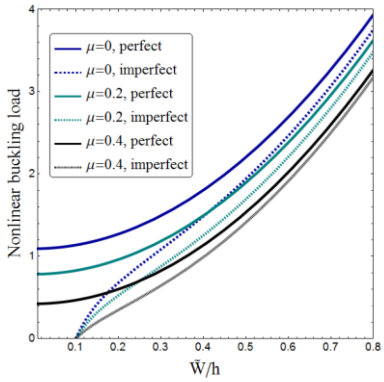


(a) S-S

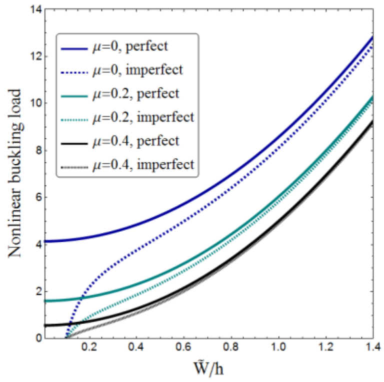


(b) C-C

Fig. 4 Nonlinear buckling path of the nanobeam against normalized deflection for different nonlocal parameters ($L/h$=10, $\xi$=0.2, $p$=1

incorporation of porosities.

Pore dispersion impact on post-buckling curves of porosity-dependent graded nano-sized beams is depicted in Fig. 3 when μ=0.2. Obtained data reveal that a nano-sized beam containing un-even pore dispersion has a larger non-linear buckling load than that containing even pore dispersion. Such behavior reveals that the nano-sized beam having un-even pores may achieve a greater beam stiffness than that containing even pore dispersion. Thus, pore dispersion possesses a notable impact on buckling properties and must be involved in buckling analysis of nano-sized beams. Based on previous explanations, pores may be randomly diffused all over the cross section of nano-sized beam in the case of even pore dispersion. But, they may vanish at cross section corners in the case of un-even pore dispersion.

Fig. 4 indicates the post-buckling curves of perfect/imperfect porosity-dependent graded nano-sized beam with respect to non-dimensional amplitude based on various nonlocality constants at $L/h$=10, $p$=1 and $\xi$=0.2. Even-type pore dispersion has been adopted. Post-buckling results for macro-size beams will be achieved by selecting μ =0. Obtained data reveal that nonlocality constant gives a decrement in stiffness and also a lower post-buckling load in the case of ideal and imperfect nano-sized beams. Hence, non-local model of a nano-sized beam may results in smaller values for buckling load than a local beam.

Impacts of slenderness ratio ($L/h$) on post-buckling curves of a porosity-dependent nano-sized beam having simply-supported boundary edges are shown in Fig. 5 when $\mu$=0.2, $\xi$=0.2. Even-type pore dispersion has been adopted. One can conclude from the figure that nano-sized beams are less flexible at smaller values of slenderness ratio. Thus, presented post-buckling loads get larger by decreasing in slenderness ratio at a prescribed non-dimensional maximum deflection.

Geometric imperfection ($W^*/h$) impacts on post-buckling curves of porosity-dependent graded nano-sized beams with even-type pore dispersion have been indicated in Fig.6 at $\mu$=0.2 and $\xi$=0.2. It is found that the initial state of nano-sized beam possesses a major impact on post-buckling properties. According to previous paragraphs, the critical buckling load vanishes by introducing initial geometric state. In fact, for perfect state ($W^*/h$=0), the nano-sized beam buckles at first. After that, nano-sized beam stiffness gets larger by increasing in non-dimensional maximum deflection. However, for imperfect state ($W^*/h\neq 0$), one cannot find any critical load before the initial configuration of the nano-sized beam.

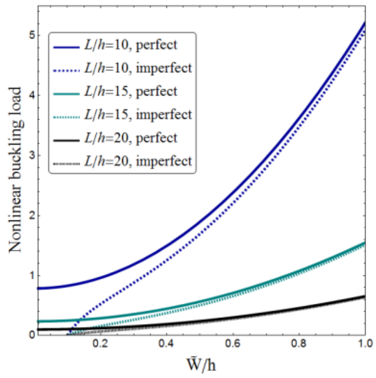


Fig. 5 Nonlinear buckling path of the nanobeam against normalized deflection for different slenderness ratios ($\mu$=0.2, $\xi$=0.2, $p$=1)

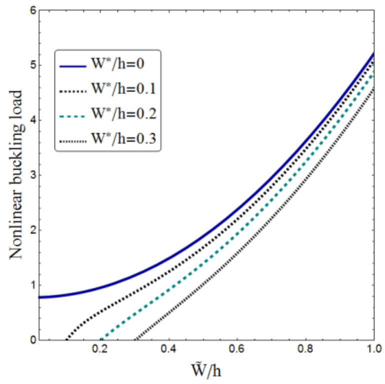


Fig. 6 Nonlinear buckling path of the nanobeam against normalized for different imperfection parameters (L/h=10, $\mu$=0.2, $\xi$=0.2, $p$=1).

## 5. Conclusions

The main purpose of this paper was analyzing nonlinear buckling response of a nonlocal porous FG beam based upon a non-linear refined thick beam formulation. The diffusion of pores inside FGM had two patterns. It was understood that increasing the nonlocal parameter led to reduction in the post-buckling load. The pore parameter or pattern of pore distribution had a great impact on post-buckling path of nano-sized beam. Post-buckling load for the state of uneven pore diffusion was bigger that of even porosities. Moreover, geometric imperfection had a notable impact on post-buckling response of porous nano-sized beam near the deflected configuration.

## References

Atmane, H.A., Tounsi, A., Bernard, F and Mahmoud, S.R. (2015), "A computational shear displacement model for vibrational analysis of functionally graded beams with porosities", *Steel Compos. Struct.*, **19**(2), 369-384.

Barati, M.R and Zenkour, A.M. (2018a), "Analysis of postbuckling behavior of general higher-order functionally graded nanoplates with geometrical imperfection considering porosity distributions", *Mech. Adv. Mater. Struct.*, 1-8.

Barati, M.R and Zenkour, A.M. (2018b), "Post-buckling analysis of imperfect multi-phase nanocrystalline nanobeams considering nanograins and nanopores surface effects", *Compos. Struct.*, **184**, 497-505.

Barati, M.R. (2017), "Nonlocal microstructure-dependent dynamic stability of refined porous FG nanoplates in hygro-thermal environments", *Eur. Phys. J. Plus*, **132**(10), 434.

Barati, M.R., Shahverdi, H. and Zenkour, A.M. (2017), "Electro-mechanical vibration of smart piezoelectric FG plates with porosities according to a refined four-variable theory", *Mech. Adv. Mater. Struct.*, **24**(12), 987-998.

Barati, M.R., Zenkour, A.M. and Shahverdi, H. (2016), "Thermo-mechanical buckling analysis of embedded nanosize FG plates in thermal environments via an inverse cotangential theory", *Compos. Struct.*, **141**, 203-212.

Belkorissat, I., Houari, M.S.A., Tounsi, A., Bedia, E.A. and Mahmoud, S.R. (2015), "On vibration properties of functionally graded nano-plate using a new nonlocal refined four variable model", *Steel Compos. Struct.*, **18**(4), 1063-1081.

Berrabah, H.M., Tounsi, A., Semmah, A. and Adda, B. (2013), "Comparison of various refined nonlocal beam theories for bending, vibration and buckling analysis of nanobeams", *Struct. Eng. Mech.*, **48**(3), 351-365.

Bouderba, B., Houari, M.S.A., Tounsi, A. and Mahmoud, S.R. (2016), "Thermal stability of functionally graded sandwich plates using a simple shear deformation theory", *Struct. Eng. Mech.*, **58**(3), 397-422.

Chen, D., Yang, J and Kitipornchai, S. (2015), "Elastic buckling and static bending of shear deformable functionally graded porous beam", *Compos. Struct.*, **133**, 54-61.

Ebrahimi, F. and Barati, M.R. (2018), "Stability analysis of porous multi-phase nanocrystalline nonlocal beams based on a general higher-order couple-stress beam model", *Struct. Eng. Mech.*, **65**(4), 465-476.

Ebrahimi, F. and Barati, M.R. (2017), "Hygrothermal effects on vibration characteristics of viscoelastic FG nanobeams based on nonlocal strain gradient theory", *Compos. Struct.*, **159**, 433-444.

Emam, S.A. (2009), "A static and dynamic analysis of the postbuckling of geometrically imperfect composite beams. *Compos. Struct.*, **90**(2), 247-253.

Eringen, A.C. (1983), "On differential equations of nonlocal elasticity and solutions of screw dislocation and surface waves", *J. Appl. Phys.*, **54**(9), 4703-4710.

Hadji, L., Daouadji, T.H and Bedia, E.A. (2015), "A refined exponential shear deformation theory for free vibration of FGM beam with porosities", *Geomech. Eng.*, **9**(3), 361-372.

Li, L and Hu, Y. (2017), "Post-buckling analysis of functionally graded nanobeams incorporating nonlocal stress and microstructure-dependent strain gradient effects", *Int. J. Mech. Sci.*, **120**, 159-170.

Li, L., Li, X and Hu, Y. (2016), "Free vibration analysis of nonlocal strain gradient beams made of functionally graded material", *Int. J. Eng. Sci.*, **102**, 77-92.

Mirjavadi, S.S., Afshari, B.M., Barati, M.R. and Hamouda, A.M.S. (2019), "Transient response of porous FG nanoplates subjected to various pulse loads based on nonlocal stress-strain gradient theory", *Eur. J. Mech. A Solids*, **74**, 210-220.

Wattanasakulpong, N. and Ungbhakorn, V. (2014), "Linear and nonlinear vibration analysis of elastically restrained ends FGM beams with porosities", *Aerosp. Sci. Technol.*, **32**(1), 111-120.

Yahia, S.A., Atmane, H.A., Houari, M.S.A. and Tounsi, A. (2015), "Wave propagation in functionally graded plates with porosities using various higher-order shear deformation plate theories", *Struct. Eng. Mech.*, **53**(6), 1143-1165.

Zemri, A., Houari, M.S.A., Bousahla, A.A. and Tounsi, A. (2015), "A mechanical response of functionally graded nanoscale beam: An assessment of a refined nonlocal shear deformation theory beam theory", *Struct. Eng. Mech.*, **54**(4), 693-710.

Zhang, L.L., Liu, J.X., Fang, X.Q and Nie, G.Q. (2014), "Effects of surface piezoelectricity and nonlocal scale on wave propagation in piezoelectric nanoplates", *Eur. J. Mech. A Solids*, **46**, 22-29.

*JS*